Temperature Profiling of VCSELs by Thermoreflectance Microscopy

M. Farzaneh, Reja Amatya, Dietrich Lüerßen, Kathryn J. Greenberg, Whitney E. Rockwell, and Janice A. Hudgings, *Senior Member, IEEE*

***Abstract*—Surface temperature measurements with submicron spatial resolution are reported for operating vertical-cavity surface-emitting lasers (VCSELs) by means of thermoreflectance microscopy. We measure increasingly convex radial temperature distributions with increasing bias power for three types of VCSELs. The corresponding convex refractive index profiles are consistent with previously observed thermal lensing; this effect is far more prominent for the oxide confined single-mode (SM) VCSEL than for the broader aperture devices. For all samples, the change in the average surface temperature varies linearly with the change in dissipated power. A comparison with the temperature of the top distributed Bragg reflector mirror of an oxide confined SM VCSEL, obtained from the wavelength shift of the spontaneous emission, shows that both methods yield comparable results.**

***Index Terms*—Temperature, thermoreflectance, vertical-cavity surface-emitting lasers (VCSELs).**

I. Introduction

THERMAL effects are known to influence the performance of vertical-cavity surface-emitting lasers (VCSELs) through local gain compression, polarization switching, variations in the threshold current, decrease in the output power, and self-focusing of the beam due to thermal lensing [1]–[5]. Therefore, it is highly desirable to accurately measure the temperature profile of an operating VCSEL in order to characterize device performance and to enable device design for improved thermal management.

The most commonly used method of measuring temperature in VCSELs by monitoring the shift in lasing wavelength [3] provides only a spatially averaged temperature, which fails to resolve lateral and longitudinal temperature variations within the laser. Alternative methods include spatially resolved monitoring of the spontaneous electroluminescence wavelength shift (μ-EL) [6] and scanning thermal microscopy (SThM) [7]. μ-EL enables measurement of the radial temperature distribution of the top VCSEL mirror, with a demonstrated spatial resolution of 1–2 μm. SThM, which has been successfully demonstrated on a cross-sectioned VCSEL, is not suitable on a light-emitting surface since the optical radiation is absorbed by the microthermocouple.

In this letter, we present two-dimensional (2-D), spatially resolved, nondestructive profiling of the surface temperature of three types of VCSELs under operating conditions, using thermoreflectance imaging. The high spatial and thermal resolutions of 250 nm and 10 mK achieved with this technique [8] are especially important in the characterization of narrow aperture VCSELs. The results are also compared with the traditional method of using wavelength shift to infer temperature for an oxide confined single-mode (SM) VCSEL.

II. Experimental Procedures

Thermoreflectance microscopy measures the normalized change in surface reflectivity ($\Delta R/R$) due to the modulation of surface temperature (ΔT)

$$\Delta T = \left(\frac{1}{R}\frac{\partial R}{\partial T}\right)^{-1}\frac{\Delta R}{R} \equiv \kappa^{-1}\frac{\Delta R}{R} \tag{1}$$

where κ is the thermoreflectance calibration coefficient, which depends on the material and wavelength. In this work, thermoreflectance measurements are performed using an experimental setup similar to that of [9] with a $100\times$, NA $= 0.8$ microscope objective and a blue ($\lambda = 467$ nm) light-emitting diode, leading to a measured spatial resolution of 250 nm. Using a 12-bit 60-Hz charge-coupled device camera as a detector enables 2-D thermal imaging. A BG-39 blue-pass filter from Chroma placed in the detection beam path nominally attenuates the laser wavelength better than 10^{-15} while transmitting around 85% of the thermoreflectance illumination. The three 850-nm VCSELs under study are an oxide confined SM VCSEL, an oxide confined multimode (MM) VCSEL, and a proton implanted MM VCSEL from Advanced Optical Components, with threshold currents of 1.1, 1.56, and 3.36 mA, respectively, as shown in Fig. 1(a).

The thermoreflectance calibration coefficient κ in (1) is determined using microthermocouples, which will absorb light emitted from the VCSEL surface. Hence, the calibration is performed by using a thermoelectric cooler to modulate the temperature of an unbiased VCSEL. Employing this method, we obtain a calibration coefficient of $\kappa = 2.3 \times 10^{-4}$ K^{-1}, which is very similar for both the oxide-confined and proton implanted VCSELs and is comparable to the previously measured values of κ for AlGaAs [10].

Surface temperature profiles of the VCSELs under operating conditions are obtained via thermoreflectance imaging. The required temperature modulation ΔT is obtained by sinusoidal

Manuscript received November 13, 2006; revised January 26, 2007. This work was supported by the National Science Foundation under Grant ECS-0134228 and Grant DMI-0531171, and by the Research Corporation.

M. Farzaneh is with the Department of Physics, Mount Holyoke College, South Hadley, MA 01075 USA, and also with the Research Laboratory of Electronics, MIT, Cambridge, MA 02139 USA (e-mail: mfarzane@mtholyoke.edu).

R. Amatya is with the Research Laboratory of Electronics, MIT, Cambridge, MA 02139 USA (e-mail: ramatya@mit.edu).

D. Lüerßen was with the Department of Physics, Mount Holyoke College, South Hadley, MA 01075 USA and the Research Laboratory of Electronics, MIT, Cambridge, MA 02139 USA. He is now with Oxford Gene Technology Ltd., Oxford, OX5 1PF U.K. (e-mail: dlueerssen@google-mail.com).

K. J. Greenberg, W. E. Rockwell, and J. A. Hudgings are with the Department of Physics, Mount Holyoke College, South Hadley, MA 01075 USA (e-mail: green20k@mtholyoke.edu; werockwe@mtholyoke.edu; jhudging@mtholyoke.edu).

Digital Object Identifier 10.1109/LPT.2007.894348

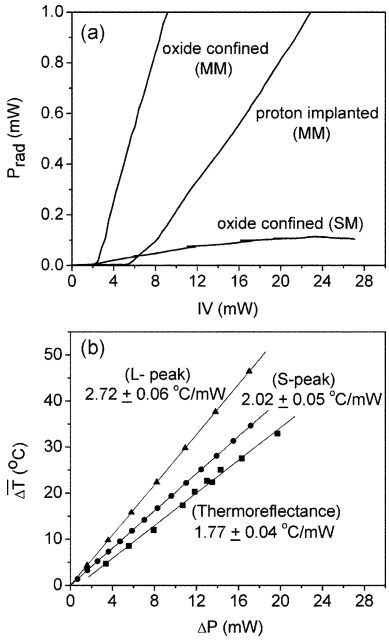

Fig. 1. (a) Radiative power $P_{\rm rad}$ as a function of electrical power IV for the three VCSELs under study. (b) Average change in temperature of the oxide-confined SM VCSEL as a function of change in dissipated power. Temperature is measured by three methods: shift in lasing wavelength (L-peak; triangles), shift in spontaneous emission peak wavelength (S-peak; circles), and thermoreflectance (squares). Lines are the linear fits to the data points.

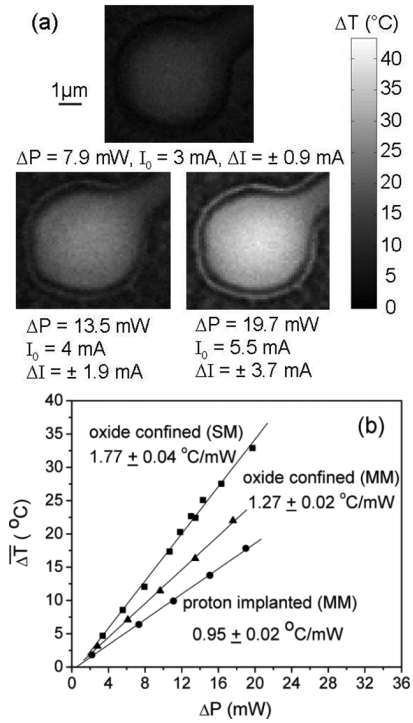

Fig. 2. (a) Typical thermoreflectance images of the oxide confined SM VCSEL at three different dissipated power values. (b) Average change of the VCSEL temperature as a function of change in dissipated power for oxide confined SM (squares), oxide confined MM (triangles), and proton implanted MM (circles) VCSELs. Lines are the linear fits to the data points.

modulation of the injection current (with various dc current levels I_0 and modulation depths ΔI) at 10 Hz while the heat sink temperature is actively controlled at 20 °C. Wavelength shift measurements are performed using a 0.1-nm resolution optical spectrum analyzer.

III. Results and Discussion

Typical thermoreflectance images of an operating oxide-confined SM VCSEL are shown in Fig. 2(a). These images show spatially resolved changes in surface temperature of the VCSEL in response to a sinusoidal modulation of the injection current. As expected, the VCSELs are hotter near the central axis than at the perimeter.

The surface temperature is governed by a simple energy balance model [11]. Since the convection losses are relatively small, the change in surface temperature ΔT should vary linearly with the modulated dissipated power $\Delta P = \Delta(IV - P_{\rm rad})$, where IV is the electrical power and $P_{\rm rad}$ is the radiated optical power, measured with a photodetector. Fig. 2(b) shows the experimentally measured change in temperature ΔT averaged over the VCSEL's surface, as a function of ΔP for the three types of VCSELs. The measured linear rate of change in temperature with dissipated power is greatest for the oxide-confined SM VCSEL (1.77 ± 0.04 °C/mW). This is consistent with the fact that this VCSEL ($\sim$5.5-μm contact aperture diameter) has a narrower oxide aperture and, therefore, a higher thermal resistance than the other two VCSELs [12]. The oxide-confined MM VCSEL has a value of 1.27 ± 0.02 °C/mW. The value of 0.95 °C/mW for the proton implanted VCSEL, which has a $\sim$15-μm contact aperture diameter, is close to the value of 0.9 °C/mW reported previously [4].

The rate of change in temperature with dissipated power measured via thermoreflectance is compared to that estimated by traditional wavelength shift measurements in Fig. 1(b). The rate of change in wavelength for the lasing peak (L-peak) and the spontaneous emission peak (S-peak) with the dissipated power (measured with respect to the threshold), $d\lambda/d(\Delta P)$, for the oxide-confined SM VCSEL is measured to be 0.173 and 0.112 nm/mW, respectively. By fixing the injected current at 4 mA and increasing the heat sink temperature, the red-shift rates of $d\lambda/d(\Delta T)$ of 0.063 nm/°C and, 0.055 nm/°C are measured for the L- and the S-peaks, respectively, which are in agreement with prior results [6]. From this analysis, a temperature increase at a rate of $d(\Delta T)/d(\Delta P) = [d\lambda/d(\Delta P)][d\lambda/d(\Delta T)]^{-1} = 2.72 \pm 0.06$ °C/mW for the L-peak and 2.02 ± 0.05 °C/mW for the S-peak is calculated.

The discrepancy in the three results in Fig. 1(b) arises because of subtle differences in what temperature is measured by each technique. Thermoreflectance measures the temperature of the VCSEL surface. The lasing wavelength is determined by the cavity resonance, so shift in lasing wavelength effectively samples the temperature of the VCSEL as a whole. The spontaneous emission feature in the optical spectrum occurs at the first zero of the reflectivity spectrum of the distributed Bragg reflector (DBR) mirror. Hence, the red-shift of the spontaneous emission peak can be used to estimate the average temperature of the top DBR mirror. The carrier density contribution to the cavity transmission spectrum is neglected, since above threshold, to the first approximation, the carrier density changes are negligible [6]. Fig. 1(b) shows that, as expected, the rate of change of the VCSEL temperature with dissipated power measured by thermoreflectance is closer to that predicted by the spontaneous

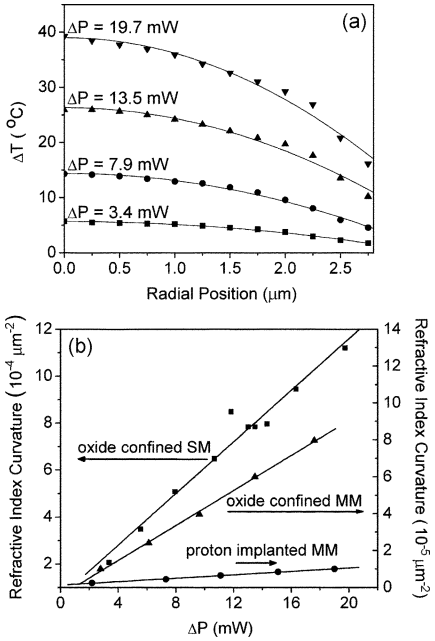

Fig. 3. (a) Radial surface temperature distribution for the oxide confined SM VCSEL at four different values of dissipated power. Lines are the parabolic fits to the data points. (b) Thermally induced refractive index curvature as a function of power for the oxide confined SM (squares), oxide confined MM (triangles), and proton implanted MM (circles) VCSELs. Lines are guides to the eye.

emission peak than to the value predicted by the shift in lasing wavelength. The results of Fig. 1(b), showing that the surface temperature is slightly lower than the DBR mirror temperature, are also evident from SThM measurements [7].

The high spatial resolution of thermoreflectance imaging enables measurement of the surface temperature distribution across the VCSEL aperture. Fig. 3(a) shows the radial surface temperature distribution of the oxide confined SM VCSEL at four different dissipated powers. These results clearly show nonuniform heating of the top mirror, with an increasingly convex thermal profile with dissipated power. At $\Delta P = 19.7$ mW, the temperature variation ΔT at the edge of the contact aperture is 40% that of the center. Using a parabolic fit to the radial temperature distributions in the form of $\Delta T(r) = C - ar^2$, a value for curvature a can be extracted. The parabolic thermal profile results in a convex radial refractive index profile, such that the top mirror of the VCSEL forms an effective graded index lens, for which the focal length varies with power. This is the so-called "thermal-lens" effect that has been observed in VCSELs [5]. By writing the radial change in refractive index as $\Delta n(r) = (\partial n/\partial T)\Delta T(r)$, and using the value of $\partial n/\partial T = 4 \times 10^{-4}$ K^{-1} for AlGaAs [13], the thermally induced refractive index curvature is calculated and plotted as a function of dissipated power in Fig. 3(b). The increase in the refractive index curvature with power is evident for all three types of VCSELs. However, this increase is about an order of magnitude larger for the narrow aperture oxide confined SM VCSEL. Since the focal length of the thermal lens is inversely proportional to the refractive index curvature, the increase in the refractive index curvature with the increase in bias power is indicative of the self-focusing phenomena in VCSELs, which is more pronounced in narrow aperture devices.

IV. Conclusion

High-resolution 2-D surface temperature profiling of three types of VCSELs by means of thermoreflectance microscopy shows a linear relationship between the surface temperature and dissipated power. The rate of increase in VCSEL surface temperature with dissipated power measured by thermoreflectance is similar to the rise in top DBR temperature predicted by the shift in the spontaneous emission wavelength. The imaged surface temperature profile shows a parabolic radial variation, with maximum heating in the center of the VCSELs. This effect is more pronounced for the SM oxide confined VCSEL, consistent with increased thermal lensing in narrow-aperture devices.

Acknowledgment

The authors would like to thank R. J. Ram and P. Mayer for useful discussions and joint development of the experimental apparatus.

References

[1] C. Degan, I. Fischer, and W. Elsäßer, "Thermally induced local gain suppression in VCSELs," *Appl. Phys. Lett.*, vol. 76, pp. 3352–3354, Jun. 2000.

[2] K. D. Choquette, D. A. Richie, and R. E. Leibenguth, "Temperature dependence of gain-guided VCSEL polarization," *Appl. Phys. Lett.*, vol. 64, pp. 2062–2064, Apr. 1994.

[3] B. Lu, P. Zhou, J. Cheng, K. J. Malloy, and J. C. Zolper, "High temperature pulsed and continuous-wave operation and thermally stable threshold characteristics of VCSELs grown by metalorganic chemical vapor deposition," *Appl. Phys. Lett.*, vol. 65, pp. 1337–1339, Sep. 1994.

[4] J. M. Catchmark *et al.*, "Extended temperature and wavelength performance of vertical cavity top surface emitting lasers," *Appl. Phys. Lett.*, vol. 63, pp. 3122–3124, Dec. 1993.

[5] M. Brunner, K. Gulden, R. Hovel, M. Moser, and M. Ilegems, "Thermal lensing effects in small oxide confined VCSELs," *Appl. Phys. Lett.*, vol. 76, pp. 7–9, Jan. 2000.

[6] M. Dabbicco, V. Spagnolo, M. Ferrara, and G. Scamarcio, "Experimental determination of the temperature distribution in trench-confined oxide VCSELs," *IEEE J. Quantum Electron.*, vol. 39, no. 6, pp. 701–707, Jun. 2003.

[7] K. Luo, R. W. Herrick, A. Majumdar, and P. Petroff, "Scanning thermal microscopy of a VCSEL," *Appl. Phys. Lett.*, vol. 71, pp. 1604–1606, Sep. 1997.

[8] P. M. Mayer, D. Lueerssen, R. J. Ram, and J. A. Hudgings, "Theoretical and experimental investigation of hte resolution and dynamic range of CCD-based thermoreflectance," *J. Opt. Soc. Amer., A*, to be published.

[9] S. Grauby, B. C. Forget, S. Hole, and D. Fournier, "High resolution photothermal imaging of high frequency phenomena using a visible charge coupled device camera associated with a multichannel lock-in scheme," *Rev. Sci. Instrum.*, vol. 70, pp. 3603–3608, Sep. 1999.

[10] S. Dilhaire, S. Grauby, and W. Claeys, "Thermoreflectance calibration procedure on a laser diode: Application to catastrophic optical facet damage analysis," *IEEE Elect. Device Lett.*, vol. 26, no. 7, pp. 461–463, Jul. 2005.

[11] K. P. Pipe and R. J. Ram, "Comprehensive heat exchange model for a semiconductor laser diode," *IEEE Photon. Technol. Lett.*, vol. 15, no. 4, pp. 504–506, Apr. 2003.

[12] M. H. MacDougal, J. Geske, C.-K. Lin, A. E. Bond, and P. D. Dapkus, "Thermal impedance of VCSELs with AlO_x-GaAs DBRs," *IEEE Photon. Technol. Lett.*, vol. 10, no. 1, pp. 15–17, Jan. 1998.

[13] N. K. Dutta, L. W. Tu, G. Hasnain, G. Zydzik, Y. H. Wang, and A. Y. Cho, "Anomalous temporal response of gain guided surface emitting lasers," *Electron. Lett.*, vol. 27, pp. 208–210, Jan. 1991.